

Induction-independent Recruitment of CREB-binding Protein to the *c-fos* Serum Response Element through Interactions between the Bromodomain and Elk-1*

Received for publication, August 28, 2000, and in revised form, November 7, 2000
Published, JBC Papers in Press, November 16, 2000, DOI 10.1074/jbc.M007824200

L. Johan Nissen‡, Jean-Christophe Gelly, and Robert A. Hipskind§

From the Institut de Génétique Moléculaire de Montpellier, IFR24, CNRS, 1919 Rte. de Mende, Montpellier 34293, France

Proliferative signals lead to the rapid and transient induction of the *c-fos* proto-oncogene by targeting the ternary complex assembled on the serum response element (SRE). Transactivation by both components of this complex, serum response factor (SRF) and the ternary complex factor Elk-1, can be potentiated by the coactivator CREB-binding protein (CBP). We report a novel interaction between the bromodomain of CBP, amino acids 1100–1286, and Elk-1. DNA binding and glutathione *S*-transferase pull-down assays demonstrate that binding requires Elk-1_{1–212} but not the C-terminal transactivation domain. Competition and antibody controls show that the bromocomplex involves both SRF and Elk-1 on the *c-fos* SRE and uniquely Elk-1 on the E74 Ets binding site. Interestingly, methylation interference and DNA footprinting analyses show almost indistinguishable patterns between ternary and bromocomplexes, suggesting that CBP-(1100–1286) interacts via Elk-1 and does not require specific DNA contacts. Functionally, the bromocomplex blocks activation, because cotransfection of CBP-(1100–1286) reduces RasV12-driven activation of SRE and E74 luciferase reporters. Repression is relieved moderately or strongly by linking the bromodomain to the N- or C-terminal transactivation domains of CBP, respectively. These results are consistent with a model in which CBP is constitutively bound to the SRE in a higher order complex that would facilitate the rapid transcriptional activation of *c-fos* by signaling-driven phosphorylation.

MAPK¹ signaling pathways that play a key role in this response by the activation of immediate early genes like the proto-oncogene *c-fos* (1). The *c-fos* promoter contains three major regulatory elements, the CaCRE, the SRE, and the SIE (2, 3). The Ca²⁺ and cAMP-response element (CaCRE) can mediate activation by cAMP-PKA or Ca²⁺-calmodulin-dependent kinase signals, which lead to phosphorylation of the transcription factor CREB on Ser-133 (4). CREB is also targeted by MAPK cascades through the activation of MAPKAP kinases (5, 6). The *v-sis*-inducible element (SIE) is targeted through cytokine- and growth factor-driven STAT1 and -3 activation (7), and their activity can be modulated by the MAPKs.

The serum response element (SRE) on the *c-fos* promoter alone is sufficient to confer a signal-dependent activation (8). Genomic footprinting studies have shown that a complex is assembled over this promoter before, during, and after induction (9). A complex with similar characteristics can be reproduced on the SRE *in vitro* by a dimer of serum response factor (SRF) and one molecule of ternary complex factor (TCF) (10). The TCFs are encoded by a family of Ets proteins that includes Elk-1, SAP-1a, and a third member variously called NET, ERP, or SAP-2 (11). Elk-1 and Sap-1a play a key role in translating signals from kinases into transcriptional activation. The TCFs represent major nuclear targets for the MAPKs ERK, p38, and SAPK. The resulting phosphorylation of TCF plays a major role in the induction of the *c-fos* gene by a mechanism that remains to be fully resolved (2).

SRE-driven transcriptional activation appears to involve co-activators of the CBP/p300-family. CBP has been described to interact with the C-terminal transactivation domains of the TCFs Elk-1 and Sap-1a and with full-length SRF (12–14). This involves the CBP region spanning aa 451–721 for TCF (12, 13) and the N-terminal CBP region spanning aa 1–1097 for SRF (14). Accordingly, CBP increases transcriptional activation by Elk-1, SAP-1a, and SRF in transient transfection assays (12–15). Thus, SRE-driven transcriptional activation appears to involve the recruitment of CBP to the ternary complex, as has also been observed for the CREB-CaCRE and STAT-SIE *c-fos* promoter complexes (16–18).

The kinetics of *c-fos* transcriptional induction suggest that the recruitment of the coactivator is either a very rapid process or that the coactivator is already present on the promoter. Here we have tested the latter possibility, namely that CBP might interact constitutively with the complex assembled over the SRE. We show that the bromodomain of CBP interacts with the TCF Elk-1 in solution and generates an Elk-1-dependent qua-

One response of cells to extracellular stimuli is the activation of signaling pathways that lead to changes in gene expression mediating proliferation, differentiation, and apoptosis. A major messenger system to these downstream events is the various

* This work was supported in part by grants from the French Association pour la Recherche sur le Cancer and Fondation pour la Recherche Médicale, as well as from the Pharma Division of Novartis, S.A. The costs of publication of this article were defrayed in part by the payment of page charges. This article must therefore be hereby marked “advertisement” in accordance with 18 U.S.C. Section 1734 solely to indicate this fact.

‡ Received support for some research costs from The Danish Research Academy.

§ To whom correspondence should be addressed: Tel.: 33-467-613-667; Fax: 33-467-040-231; E-mail: hipskind@jones.igm.cnrs-mop.fr.

¹ The abbreviations used are: MAPK, mitogen-activated protein kinase; CaCRE, calcium- and cAMP-responsive element; SRE, serum response element; SIE, *v-sis*-inducible element; PKA, protein kinase A; CREB, cAMP response element binding protein; MAPKAP, mitogen-activated protein kinase-activated protein kinase; STAT, signal transducer and activator of transcription; SRF, serum response factor; TCF, ternary complex factor; ERK, extracellular signal-regulated kinase; SAPK, stress-activated protein kinase; CBP, CREB binding protein; aa, amino acid(s); DMEM, Dulbecco's modified Eagle's medium; GST, glu-

tathione *S*-transferase; PAGE, polyacrylamide gel electrophoresis; Sarkosyl, *N*-lauroyl sarcosine; PCR, polymerase chain reaction; BSA, bovine serum albumin; wt, wild type; coreSRF, SRF-(90-245); FAP, *c-fos* AP1-like element.

ternary complex *in vitro* on the SRE. A similar Elk-1-dependent complex forms on the E74 site bound directly by Elk-1. Moreover, this novel complex represses transcriptional activation of SRE and E74 reporter genes driven by RasV12, whereas activity is restored by including the C- and N-terminal activation domains of CBP. These data suggest a model where the bromodomain anchors CBP to the SRE via TCF in a higher order complex. This would facilitate the rapid transcriptional activation of *c-fos* mediated by CBP through interaction with transcription factors targeted by signaling-driven phosphorylation.

EXPERIMENTAL PROCEDURES

Materials—Restriction enzymes were obtained from Life Technologies and New England BioLabs. Antibodies against the DNA binding domain of Gal4 were purchased from CLONTECH and Santa Cruz Biotechnology, Inc., rat monoclonal antibodies to hemagglutinin were from Roche Molecular Biochemicals, and the Elk-1 antibody against the Ets domain (aa 1–82) of Elk-1 (α -Ets) and the SRF antibody (NOP-13) have been described previously (19, 20). Horseradish peroxidase-coupled secondary antibodies were from Sigma-Aldrich. Glutathione-Sepharose, poly (dI-dC)(dI-dC), ECL-plus nitrocellulose membranes, and the T7 DNA polymerase sequencing kit were purchased from Amersham Pharmacia Biotech, whereas Talon metal-affinity resin came from CLONTECH. Transfast transfection reagent, a TnT-coupled *in vitro* transcription translation kit, *Taq* DNA polymerase, and the Dual Luciferase kit were purchased from Promega. Radioisotopes, ECL reagents, and polyvinylidene difluoride were obtained from PerkinElmer Life Sciences. Immobilon-P polyvinylidene difluoride membrane was from Millipore. DMEM and Dulbecco's PBS and FBS were purchased from Life Technologies. X-ray films and intensifying screens were purchased from Kodak, and B-Per reagent was purchased from Pierce. Nucleobond AX plasmid purification cartridges and the NucleoSpin extract kit were obtained from Machery-Nagel, and Jetstar plasmid cartridges came from Q-biogene. Protease and phosphatase inhibitors were from Sigma; all other ultra-pure biochemicals were from AppliChem (Darmstadt, Germany).

Plasmids—The Gal4-CBP and GST-CBP subclones have been previously described (12, 13). The Gal4-CBP-(1–1460) construct was generated by insertion of the N-terminal portion of CBP into the *SalI* and *NarI* sites of the Gal4-CBP-(1100–1460) subclone. The Gal4-CBP-(1100–2441) construct was generated by insertion of the C-terminal fragment of CBP into the *BamHI* and *NarI* sites of the Gal4-CBP-(1100–1460) subclone. The Elk-1 expression vector used for *in vitro* transcription (aa 1–428) was previously described (21). The Elk-1 N-terminal (aa 1–308) and C-terminal aa (Δ 14–308) expression vectors for *in vitro* transcription were generated by digesting the corresponding bacterial expression constructs and subcloning them into the pCal-n vector (Stratagene). The 3xSRE-, 1xEL-, and 3xEL-*fos* TATA-luciferase reporter genes were kindly provided by G. Bilbe (Novartis Pharma, Basel, Switzerland). The 4xEL-*fos* TATA-luciferase reporter construct was generated in this vector by inserting an *NotI-SpeI* fragment containing four tandem copies of the E74 sequence (21). The RasV12 and SV40 renilla luciferase expression vectors were kindly provided by A. Philips (Institut de Génétique Moléculaire de Montpellier, Montpellier, France) and a CBP_{wt} expression vector by R. Janknecht (Department of Biochemistry, Mayo Clinic, Rochester, MN). The original mouse CBP_{wt} expression vector used for the GST- and Gal4-CBP constructs (12, 13) contained a stop codon after aa 1286 leading to truncated proteins from the original clones spanning this region. Therefore the vectors originally described as GST-CBP-(1100–1460) and Gal4-CBP-(1100–1460) actually express a protein containing CBP amino acids 1100–1286 and are labeled accordingly. Plasmids were purified using cartridge systems for *in vitro* manipulations and by double banding in CsCl for transfections.

PCR Amplification and Cloning of the CBP Bromodomain—The oligos 5'-AGTCGAATTCGAGGAGCTACGCCAGGCACTTATGC-3' (upper strand) and 5'-AGCTAAGCTTCTAAGACTGCATGACAGGGTCAATT-3' (lower strand) were used to generate a fragment of CBP spanning the bromodomain (aa 1089–1196) flanked by *EcoRI* and *HindIII* sites to facilitate cloning into expression vectors. The 25- μ l PCR reactions contained 2 ng of CBP_{wt} expression vector, 300 nM of each oligonucleotide, 200 nM dNTPs, 1.5 mM MgCl₂, the supplier's reaction buffer (Promega), and 5 units of *Taq* polymerase. After 4 min at 95 °C, amplification was carried out for 24 cycles (0.5 min, 95 °C; 0.5 min, 55 °C; 0.5 min, 72 °C). The fragments were purified using a NucleoSpin extract kit, digested with *EcoRI* and *HindIII*, and then purified from an agarose gel using the NucleoSpin kit. After cloning into Blue-

script KS+ (Stratagene), positive clones were confirmed by sequencing. The bromodomain-encoding fragment was recloned into pGEX-2T-6His and clones screened for expression of the GST-bromo fusion protein, as well as into pCDNA3.1-FLAG. This vector was used to confirm bromodomain expression by coupled *in vitro* transcription translation (see below).

Purification of Bacterially Expressed Recombinant Proteins—*Escherichia coli* strain BL21(LysE) was electroporated with the appropriate expression vector. Fresh colonies were used to inoculate 200-ml bacterial cultures, which were grown at 37 °C, and recombinant protein expression induced in exponential phase by adding isopropyl thiogalactoside to 0.1 mM. After 1–4 h at 37 °C, bacteria were collected by centrifugation and lysed in 10 ml of B-Per reagent according to the supplier's recommendations. Insoluble proteins were removed by centrifugation at 27,000 $\times g$ for 15 min at 4 °C. The supernatant was brought to 1 mM imidazole and incubated overnight with 50–200 μ l of Talon resin at 4 °C. The mix was poured into a column, the resin was washed twice with 5 ml of RJD* buffer (10 mM HEPES, pH 7.9, 5 mM MgCl₂, 50 mM NaCl, 17% glycerol, 0.1 mM EDTA, 1 mM dithiothreitol, 0.05% Nonidet P-40) containing 1 mM imidazole and freshly added protease inhibitors (2.5 μ g/ml aprotinin, leupeptin, pepstatin, 0.5 mM benzamide, 0.5 mM phenylmethylsulfonyl fluoride). Recombinant His-tagged proteins were eluted with two column volumes of RJD* buffer containing 200 mM imidazole, pH 7.6, and stored in aliquots at –70 °C.

In Vitro Translation—³⁵S-Labeled Elk-1 proteins were synthesized from Bluescript KS+ vectors encoding Elk-1-(1–428), Elk-1-(1–307), or Elk-1-(308–428) by coupled *in vitro* transcription/translation in the presence of L-[³⁵S]methionine (1000 Ci/mmol) using TnT kits according to the supplier's recommendations. C-terminal truncated proteins were produced identically, using the Elk-1-(1–428) vector digested with the following restriction enzymes: *XbaI* (Elk-1-(1–428)), *BsmI* (Elk-1-(1–374)), *ApaI* (Elk-1-(1–253)), *StuI* (Elk-1-(1–212)), and *NspI* (Elk-1-(1–122)).

Pull-down Assays—Recombinant proteins purified by metal affinity chromatography were directly bound to glutathione-Sepharose beads at 4 °C for 1 h. The beads were then washed three times with a 100-fold excess of RJD*-buffer containing protease inhibitors and stored short-term at 4 °C. 5 μ l of the *in vitro* translated Elk-1 proteins described above were added to 10 μ l of a 50% slurry of protein-bearing beads in a total volume of 100 μ l of RJD* buffer containing protease inhibitors and incubated with gentle agitation at 4 °C for 4 h. After three washes with 500 μ l of RJD*, the beads were collected, resuspended in 20 μ l of 5 \times Laemmli buffer (0.25 M Tris-HCl, pH 6.8, 10% SDS, 10% glycerol, 5% 2-mercaptoethanol, 0.001% bromophenol blue) and denatured for 5 min at 95 °C, and the bound proteins were analyzed by SDS-polyacrylamide gel electrophoresis. Proteins were visualized by Coomassie Blue staining, followed by autoradiography of the dried gels.

Immunoblotting—Proteins were subjected to electrophoresis on 6–10% SDS-PAGE minigels. Proteins larger than 100 kDa were transferred to nitrocellulose membranes by immersion blotting, whereas smaller proteins were immobilized on either nitrocellulose or polyvinylidene fluoride membranes by semi-dry transfer. Membranes were blocked with 5% dry milk in TBST (50 mM Tris-HCl, pH 7.5, 140 mM NaCl, 3 mM KCl, and 0.05% Tween 20) and then incubated with the indicated primary antibody diluted 1:1000 into the blocking buffer. After washing in TBST (6 \times 5 min), the membranes were incubated with the appropriate secondary antibody coupled to horseradish peroxidase diluted in blocking buffer. The membranes were again washed in TBST as above, and the immune complexes were visualized by enhanced chemiluminescence.

Transient Transfection and Luciferase Assays—NIH3T3 cells were maintained in DMEM containing 10% fetal bovine serum, 100 units/ml penicillin, 100 μ g/ml streptomycin. Cells were seeded to 30% confluency in 6-well plates 16 h prior to transfection. The medium was changed 1 h before transfection, which was performed using a classical Ca₂PO₄ protocol (22). The transfection mixes contained 300 ng of Luciferase reporter construct, 1 μ g of Gal4-CBP expression vector, 200 ng of RasV12 expression vector, 5 ng of pSV-Renilla Luciferase expression vector, and 3.5 μ g of pUC18. These optimal values were determined experimentally several times. Cells were washed in phosphate-buffered salt solution 8–10 h after transfection and maintained in serum-free DMEM for 40 h. Cell extracts were prepared, and luciferase activity was determined following the protocol supplied with the Dual Luciferase kit (Promega). Measurements were made in duplicate using a Berthold Lumat LB950. For protein overexpression, COS-7 cells were transfected using Transfast (Promega) according to the supplier's protocol, and whole cell extracts were prepared as described (23). Protein concentrations were determined using Bradford's reagent with BSA as

a standard. Protein expression was confirmed using immunoblotting prior to gel retardation analyses.

Gel Retardation Analysis—Probes for binding analyses were prepared from subcloned SRE (20), EL (10), and E74 sequences (21) by Klenow enzyme-catalyzed end labeling of an *EcoRI-NarI* fragment in the presence of 50 μCi of [α - ^{32}P]dATP (3000 Ci/mmol, 10 $\mu\text{Ci}/\mu\text{l}$) and 300 μM dTTP (23). The labeled fragments were purified from acrylamide gels by electroelution. The gel retardation experiments were carried out as previously described (23). In brief, reactions (7.5 μl) contained 4 fmol of labeled probe, a salt/protein/buffer mix, 2.5 μg of poly (dI-dC)·(dI-dC), recombinant coreSRF-(90–245) with SRE probes, and the proteins indicated in the figures. Where appropriate, 0.5–1 μl of antibodies was added to the reaction before the addition of protein extracts. After incubation for 30 min at room temperature, complexes were resolved on a 5% polyacrylamide gel containing 0.5 \times TBE at 1 mA/cm for 4 h. Complexes were visualized by autoradiography and phosphorimaging of the dried gel.

Methylation Interference Analysis—SRE probes were prepared from the same site described above but cloned into pUC18 at the *XbaI* site. After digestion with *HindIII-XmaI*, the upper and lower strands were end-labeled using Klenow enzyme, 300 μM dGTP, and either 50 μCi of [α - ^{32}P]dATP (3000 Ci/mmol, 10 $\mu\text{Ci}/\mu\text{l}$) for the *HindIII* end or 50 μCi of [α - ^{32}P]dCTP (3000 Ci/mmol, 10 $\mu\text{Ci}/\mu\text{l}$) for the *XmaI* end. The gel-purified fragment was treated for 3.5 min at 22 $^{\circ}\text{C}$ with 1% dimethyl sulfate in 60 mM NaCl, 10 mM Tris-HCl, pH 8.0, 1 mM EDTA. Reactions were stopped as described previously (24), and the probes were subjected to several rounds of alcohol precipitation. Binding reactions were prepared and analyzed as for gel retardation analysis except that all components were increased 5-fold. The complexes were visualized by autoradiography of the wet gel. Regions of the gel corresponding to different complexes and free DNA were electrotransferred to DEAE paper (NA45, Schleicher and Schuell) and eluted in 0.5 M NaCl, 0.5% SDS, 20 mM Tris-HCl, pH 8.0, 0.5 $\mu\text{g}/\text{ml}$ Proteinase K at 65 $^{\circ}\text{C}$. The eluted fragments were purified by organic extraction followed by ethanol precipitation. The fragments were incubated for 40 min at 95 $^{\circ}\text{C}$ in freshly made 1 M piperidine, and the piperidine was removed by multiple rounds of lyophilization and resuspension in H_2O . The samples were finally resuspended in formamide dye mix (0.3% each bromophenol blue and Xylene Cyanol FF; 10 mM EDTA, pH 7.5, 80% deionized formamide), denatured for 5 min at 95 $^{\circ}\text{C}$, and analyzed by denaturing electrophoresis in a 10% polyacrylamide-8.5 M urea sequencing gel. The gel was dried, and radioactivity was visualized by autoradiography at -70°C with an intensifying screen and phosphorimaging as described above.

Footprint Analysis—Preparative reactions were carried out as described above but incubated for 30 min at 4 $^{\circ}\text{C}$. Reactions were brought to 2.5 mM CaCl_2 , 7.5 mM MgCl_2 were attained and incubated with 0.01 unit of DNaseI at 37 $^{\circ}\text{C}$ for 1.5 min. The reaction was terminated by adding 100 μl of 0.01% Sarkosyl, 0.1 M Tris-HCl, pH 8.0, 0.1 M NaCl, 0.02 mM EDTA, 0.03 $\mu\text{g}/\mu\text{l}$ calf thymus DNA, and 0.075 $\mu\text{g}/\mu\text{l}$ Proteinase K, incubated an additional 15 min at 37 $^{\circ}\text{C}$ followed by 5 min at 95 $^{\circ}\text{C}$. Labeled DNA was purified by organic extraction and alcohol precipitation, resuspended in formamide dye mix, denatured again, and analyzed on 10% sequence gels as described above.

RESULTS

Expression of Gal4- and GST-CBP Fusion Proteins—To investigate the interactions between Elk-1 and CBP in detail, different subdomains of CBP were fused to the Gal4 DNA binding domain for expression in mammalian cells and to glutathione transferase to facilitate purification after overexpression in bacteria (12, 13). The different expression constructs are presented schematically in Fig. 1A. Immunoblotting with a Gal4-DNA binding domain antibody showed that the various fusion proteins were expressed at different levels after transient transfection of COS-7 cells (Fig. 1B). Similarly, variable amounts of the various GST fusion proteins were obtained after affinity purification of bacterially expressed proteins (Fig. 1C, lower panel). These assays were used to determine the functional protein concentration for subsequent experiments. It should be noted that the fusion proteins encoded by Gal4-CBP-(1100–1460) (12, 13) are truncated due to the presence of a stop codon after aa 1286 in the original CBP expression vector. Therefore, this protein contains the bromodomain of CBP but not the histone acetyltransferase domain immediately down-

stream and will subsequently be labeled CPB-(1100–1286).

Interaction in Solution between CBP Fusion Proteins and Elk-1—We first tested for solution interactions between various regions of CBP and Elk-1. Recombinant, bacterially produced GST-CBP fusion proteins were immobilized on glutathione-agarose beads and incubated with ^{35}S -labeled Elk-1 (aa 1–428) produced by coupled *in vitro* transcription/translation (Fig. 1C). Two versions of Elk-1 are produced *in vitro*, the smaller of which arises from internal initiation of translation at Met-55 (also see below) (25). Both full-length and N-terminal truncated Elk-1 bound to CBP-(451–721), which has previously been shown to interact with the C-terminal activation domain of Elk-1 (13). Full-length and N-terminal truncated Elk-1 also interacted with CPB-(1100–1286), which spans the bromodomain, and CBP-(1460–1891), which contains most of the histone acetyl transferase domain. The increased yield of the truncated version of Elk-1 versus that of full-length Elk-1, particularly in respect to their relative levels in the reaction input (left lane), suggests that these two CBP domains bound preferentially to N-terminal truncated Elk-1 in solution. Neither version of Elk-1 interacted with GST alone (Fig. 1C) or with other domains of CBP (not shown), nor did we detect any binding of SRF produced *in vitro* to CBP (not shown).

We then investigated the solution interaction between the bromodomain of CBP and different portions of Elk-1. To this end, *in vitro* translated ^{35}S -labeled full-length (aa 1–428), N-terminal (aa 1–307), and C-terminal (aa 308–428) Elk-1 were used as above (Fig. 1D). Similar to full-length Elk-1, the N-terminal construct gave rise to two translation products *in vitro*, unlike the C-terminal construct. This further supports the notion that the smaller form of Elk-1 arises from internal initiation of translation and not premature termination. Once again, full-length Elk-1 bound to the bromodomain of CBP in solution, as did Elk(NT), with some preference shown for the truncated version (compare bound lanes to input). CBP-(1100–1286) also interacted with *in vitro*-translated C-terminal domain of Elk-1. Interestingly this interaction appears to be independent of its activation by phosphorylation, because Elk-(308–428) is not phosphorylated during *in vitro* translation. In contrast to these interactions, none of these proteins bound to GST alone (Fig. 1D). Thus we can detect complexes between multiple domains of CBP, in particular the bromodomain, and Elk-1 in solution.

To confirm that the bromodomain alone (CBP aa 1089–1196) accounts for binding to Elk-1, an expression vector for GST-CBP-(1089–1196) was generated by PCR. This protein showed interactions with Elk(FL) and Elk(NT) that were indistinguishable from CBP-(1100–1286) (Fig. 1E) and in fact showed binding to progressively truncated versions of Elk until the region between amino acids 212 and 122 was deleted (Fig. 1E). This indicates that the region in Elk-1 spanning aa 122 to 212 is important for interaction in solution with the CBP bromodomain.

The Bromodomain of CBP Forms DNA-dependent Complexes with Elk-1 on the Consensus Ets-binding Site E74—The interactions in solution between the bromodomain of CBP and the TCF Elk-1 led us to test for similar interactions in the context of DNA-bound complexes, using the E74 Ets sequence to which Elk-1 binds directly as a monomer (21). To this end we employed extracts from COS-7 cells, transiently transfected with expression vectors for different Gal4-CBP fusions, and analyzed complex formation on a ^{32}P -labeled E74 oligonucleotide. Endogenous Elk-1 forms a characteristic complex in nontransfected cell extracts and those containing Gal4-CBP-(1–451) (Fig. 2A, lanes 1 and 2). However, cell extracts containing the bromodomain of CBP (aa 1100–1286) present a novel complex,

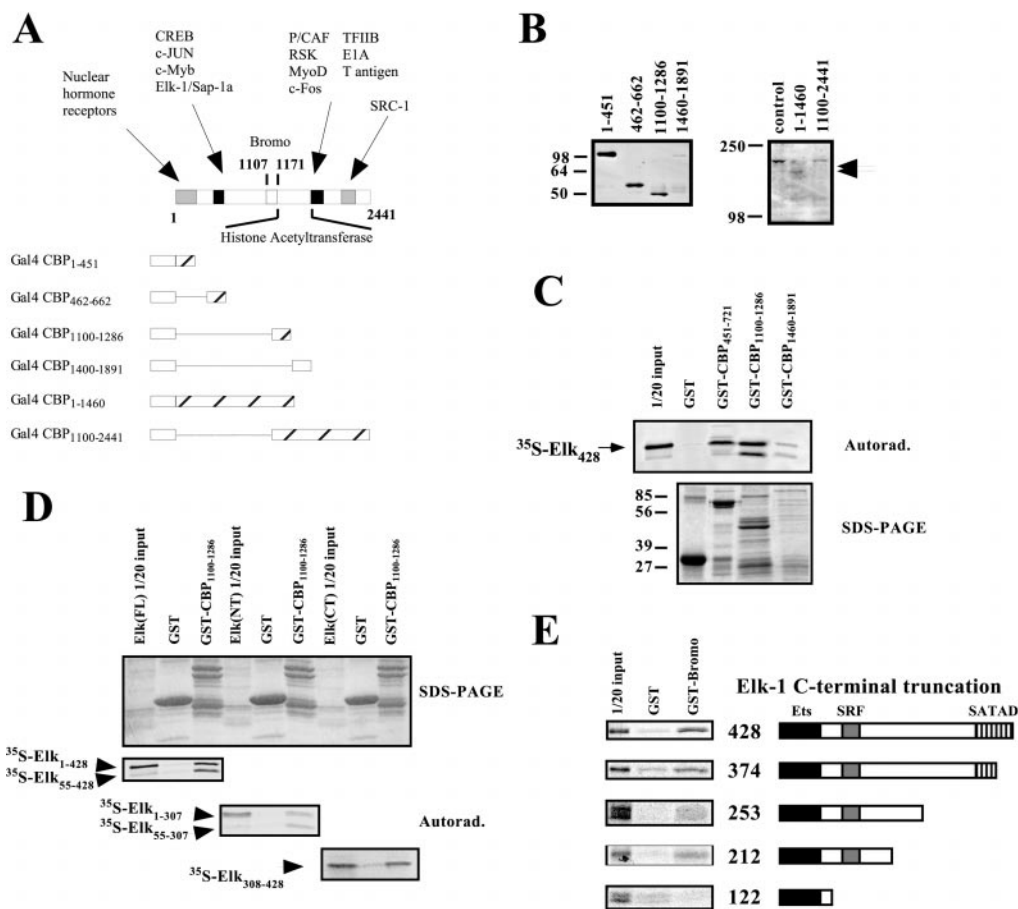


FIG. 1. The bromodomain of CBP interacts with Elk-1 *in vitro*. *A*, schematic diagram of CBP and the different regions (striped boxes) fused to the Gal4 DNA binding domain (unfilled box). The different functional domains of CBP are indicated, as are the proteins described to interact with them. The numbers correspond to the codon positions in CBP. *B*, expression of various Gal4-CBP fusion proteins. COS-7 cells were transfected with the Gal4-CBP-fusions indicated above the lanes. 25 μ g of whole cell extract were analyzed by immunoblotting using an antiserum specific for the Gal4 DNA binding domain (CLONTECH). *C*, the bromodomain of CBP interacts with Elk-1 in solution. Pull-down assays were performed using glutathione-agarose beads bearing GST or the GST-CBP fusion indicated above the lanes and full-length Elk-1 produced by *in vitro* translation (35 S-Elk₄₂₈). The reactions were separated on 10% SDS-PAGE, and Elk was detected by autoradiography of the dried gel (upper panel). An aliquot of the 35 S-Elk₄₂₈ input was loaded as control (1/20 input, left lane). The lower panel shows a Coomassie Blue-stained SDS-PAGE of the GST proteins. *D*, both the N-terminal and C-terminal domains of Elk-1 bind to the bromodomain in solution. Reactions were performed and analyzed as described in *C*, using glutathione-agarose beads bearing GST or GST-CBP-(1100–1286). The different versions of 35 S-Elk were produced by *in vitro* translation: full-length Elk-1 (FL, amino acids 1–428), the N-terminal 307 amino acids of Elk-1 (NT), and the C-terminal transactivation domain of Elk-1 (CT, amino acids 308–428). Note that FL and the NT vectors generate isoforms of Elk that start at Met-1 and at Met-55, as indicated at the side of each autoradiogram (lower panels) (25). The upper panel shows the Coomassie Blue-stained protein gel. *E*, mapping of the N-terminal region of Elk-1 that interacts with the CBP bromodomain. Agarose beads were loaded with GST or GST-CBP-(1089–1196), which contains exclusively the bromodomain and thus is labeled GST-Bromo. The 35 S-Elk-1 C-terminal truncated proteins are indicated schematically at the right. The number corresponds to the C-terminal amino acid. The panels show the appropriate portion of the autoradiogram of the pull-down assay performed as described in *C*. 1/20 input denotes the aliquot of the 35 S-Elk used in each reaction loaded as a control (left lanes). We note that each mutant also generates a second isoform that starts at Met-55, which is not shown. Ets, the Ets DNA binding domain, aa 1–90; SRF, the B domain that interacts with SRF, aa 148–168; SATAD, the signaling-activated transactivation domain, aa 308–428.

termed the bromocomplex, with slightly faster mobility than the Elk-E74 binary complex (Fig. 2A, lane 3).

Because we did not cotransfect the cells with an Elk-1 expression vector, this complex could reflect direct binding by the bromodomain of CBP. However, the bromocomplex is sensitive to a limiting concentration of an Elk-1 Ets-domain antibody but is unaffected by an antibody specific for SRF (lanes 7 and 8, also see below), indicating that the complex contains Elk-1 and is not due to direct binding to the site by the bromodomain. Notably, the addition of recombinant Elk-(308–428) had no effect on complex formation (lane 6), suggesting that complex formation involves the N-terminal domain of Elk-1. Accordingly, GST-Elk_{1–308} binds to the probe directly and also generates a novel, slower migrating complex with Gal4-CBP-(1100–1286) (lane 5). To confirm this interpretation, we performed the same test using Elk-(1–253), Elk-(1–212), and Elk-(1–122) produced *in vitro* by coupled transcription-translation. Elk-(1–253) and Elk-(1–212), but not Elk-(1–122), also formed a novel com-

plex that migrated more slowly than the bromocomplex formed with endogenous Elk-1 (Fig. 2B), as well as much more slowly than the direct complexes formed by these proteins (not shown) (21). Thus the same domain of Elk-1 is required for interaction in solution and in the context of DNA binding. These data suggest that bromocomplex formation is due to direct interaction between Elk-1 and the bromodomain of CBP, and that this can be attributed to the first 212 aa of Elk.

The Bromodomain of CBP Forms a Quaternary Complex on the c-fos SRE Together with Elk-1 and SRF—Elk-1 can interact with the *c-fos* SRE only in the presence of SRF (20), forming a ternary complex that consists of Elk-1, a dimer of SRF, and the SRE. We tested whether the bromocomplex could also be observed in this context. As above, we used extracts from COS-7 cells, transiently transfected with expression vectors for the different Gal4-CBP fusions, and analyzed ternary complex formation on the SRE. To better visualize the TCF complexes, the experiments contained coreSRF, a truncation mutant that

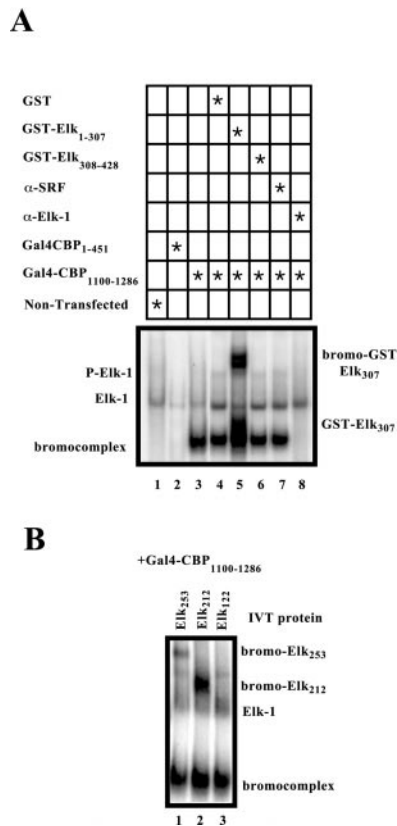


FIG. 2. The bromocomplex forms with Elk-1 alone on the E74 Ets protein binding site. *A*, gel retardation analysis of complexes formed on a ^{32}P -labeled E74 probe by 10 μg of whole cell extract from nontransfected COS-7 cells (lane 1) or cells transfected with expression vectors for Gal4-CBP-(1–451) (lanes 2) or Gal4-CBP-(1100–1286) (lanes 3–8). The following reagents were added as indicated above each lane: lane 4, 1 μg of purified GST protein; lane 5, 1 μg of purified GST-Elk₃₀₇; lane 6, 1 μg of purified GST-Elk-(308–428); lane 7, 0.5 μl of anti-SRF antiserum; lane 8, 0.5 μl of anti-Elk Ets domain antiserum. The panel shows the relevant region of the autoradiogram of the dried polyacrylamide gel. The bromocomplexes together with the noninduced and induced Elk-1 (*P-Elk*) complexes are indicated on the left, and the GST-Elk₃₀₇ and Bromo-GST Elk₃₀₇ complexes are on the right. A non-specific complex comigrates with the noninduced Elk-1 complex that is unaffected by the Elk-specific antiserum. *B*, gel retardation experiments were performed as in *A*, using whole cell extracts from COS-7 cells transfected with Gal4-CBP-(1100–1286) and Elk-1 C-terminal truncation mutants Elk₂₅₃, Elk₂₁₂, and Elk₁₂₂ produced by *in vitro* translation (see Fig. 1). The panel shows the relevant region of the autoradiogram of the dried polyacrylamide gel. The different complexes are indicated on the right.

spans aa 90–245 and contains the MADS box domain necessary for dimerization, DNA binding and ternary complex formation. The nontransfected extract shows the normal pattern of a coreSRF binary complex and a slower migrating ternary complex containing Elk-1, the major species of TCF in these cells (Fig. 3A, lane 1; see below), as does an extract from cells transfected with Gal4-CBP-(1–451) (Fig. 3A, lane 2) or Gal4-CBP-(462–662) (Fig. 3B, even-numbered lanes). Cell extracts containing the bromodomain of CBP (aa 1100–1286) present, in addition to the ternary complex, a novel faster migrating bromocomplex (Fig. 3A, lane 3; Fig. 3B, lanes 3, 5, and 7). In contrast, the bromocomplex formed upon adding full-length recombinant SRF migrates more slowly than the ternary complex (not shown), indicating a surprisingly compact structure of the bromocomplex formed with endogenous Elk-1 and coreSRF. The complex was observed in both nonstimulated and stimulated extracts, showing that this interaction is independent of Elk-1 phosphorylation (not shown).

We next characterized the bromocomplex using antibodies

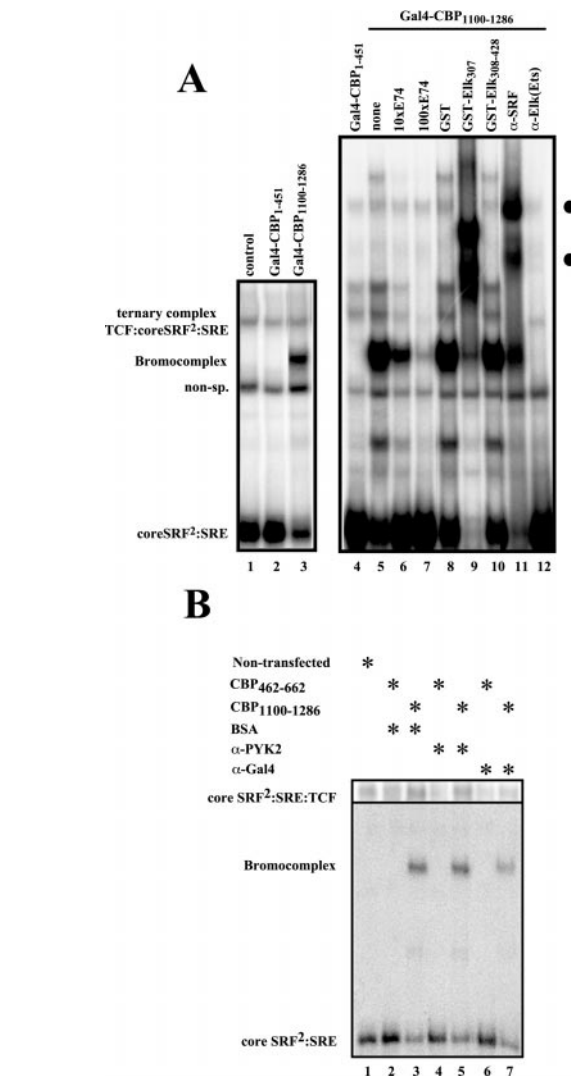


FIG. 3. The bromodomain of CBP forms a novel complex with TCF and coreSRF on the *c-fos* SRE. *A*, gel retardation analysis of complexes formed on a ^{32}P -labeled SRE probe by the SRF deletion mutant coreSRF-(90–245) and 10 μg of whole cell extract from nontransfected COS-7 cells (lane 1) or cells transfected with expression vectors for Gal4-CBP-(1–451) (lanes 2 and 4) or Gal4-CBP-(1100–1286) (lanes 3, 5–12). The following reagents were added as indicated above each lane: lanes 6 and 7, 10- and 100-fold excesses of double-stranded E74-binding site oligonucleotide; lane 8, 1 μg of purified GST protein; lane 9, 1 μg of purified GST-Elk₃₀₇; lane 10, 1 μg of purified GST-Elk-(308–428); lane 11, 0.5 μl of anti-SRF antiserum; lane 12, 0.5 μl of anti-Elk Ets domain antiserum. The panel shows the relevant region of the autoradiogram of the dried polyacrylamide gel. The coreSRF-(90–245)-SRE binary complex, the TCF:coreSRF-(90–245)-SRE ternary complex and bromocomplexes are indicated on the left, and the complexes supershifted by SRF antiserum are on the right (filled circles). *B*, the bromocomplex is partially blocked by an antiserum directed against the Gal4 DNA binding domain. Complexes were assembled as in *A* using whole cell extracts from nontransfected COS-7 cells or cells transfected with either Gal4-CBP-(1100–1286) or Gal4-CBP-(462–662) expression vectors. As indicated above the lanes, reactions also contained either BSA, anti-Pyk2 antiserum, or anti-Gal4 DNA binding domain antiserum (Santa Cruz Biotechnology). The upper panel shows the induced TCF complex from a longer exposure of the same gel. The identities of the different complexes are indicated to the left of the autoradiogram.

specific for different components of the ternary complex. These reactions contained extracts from COS-7 cells transfected with Elk-1- and Gal4CBP-(1100–1286) to amplify the ternary- and bromocomplexes. The bromocomplex is supershifted by an anti-SRF antibody (Fig. 3A, lane 11) and blocked by the Ets domain-specific Elk-1 antiserum that blocks complex formation (Fig. 3A, lane 12). This indicates that both ternary complex compo-

nents contribute to formation of the bromocomplex. Because antibodies directed against this domain of CBP are not available, we used a Gal4 antibody to target the CBP component. An antiserum directed against the DNA binding domain of Gal4 significantly reduces bromocomplex formation, unlike BSA or another antiserum from the same source (Fig. 3B, compare lanes 3, 5, and 7). The Gal4 antiserum also slightly diminishes ternary complex formation but to a lower extent than the bromocomplex (Fig. 3B, upper panel). These data show that the bromocomplex contains a protein bearing the Gal4 DNA binding domain. Because the bromocomplex does not form with other Gal4-CBP fusion proteins, it also requires the bromodomain of CBP. It is unclear why the Gal4 antiserum does not completely block or supershift the bromocomplex, although this correlates with our difficulty in using this antibody for immunodetection of Western blots (not shown).

An excess of purified recombinant GST-Elk-1(1–307) drives formation of several distinct complexes and competes for the bromocomplex formed by transfected cell extracts (Fig. 3A, lane 9). This is not the case when adding an excess of GST-Elk-1(308–428) or GST alone (Fig. 3A, lanes 8 and 10). These data indicate that, as with the E74 probe, the bromocomplex requires the Elk N-terminal domain, and that any complex formed between GST-Elk-1(1–307) and Gal4-CBP(1100–1286) shows a slower migration relative to transfected wt Elk-1. We did not detect bromocomplexes in the absence of coreSRF (not shown), nor did we detect them using a SRE probe with a mutated TCF-binding site (EL), which nevertheless showed normal coreSRF·SRE binary complexes (not shown). Thus Elk-1 is required for the bromocomplex, and the bromodomain of CBP cannot facilitate and stabilize Elk-1 binding to the SRE in the absence of SRF.

Methylation Interference and DNA Footprinting Analysis of the Bromocomplex—We used methylation interference and DNA footprinting to determine whether the bromocomplex made protein-DNA contacts beyond those of the Elk-coreSRF ternary complex, especially because the Gal4 DNA binding domain antibody partially blocked bromocomplex formation. For methylation interference, SRE probes with either the upper or lower strand ³²P-labeled were partially methylated with dimethyl sulfate and then used in preparative band shift analyses. The DNA was purified from different complexes, subjected to piperidine cleavage, and then analyzed by denaturing gel electrophoresis. Somewhat surprisingly, the sensitivity of the bromocomplex to methylation is indistinguishable from that of the ternary complex on both the upper and lower strands (Fig. 4). Thus, the bromocomplex shows no strict requirement for G or A residues outside the TCF binding site. Moreover, it does not reproduce the pattern observed on the *c-fos* AP1-like element, or FAP, in genomic footprints prior to and during induction (9).

The lack of any apparent difference in methylation pattern led us to analyze the bromocomplex by DNaseI footprinting. Solution binding reactions were assembled using SRE probes labeled on the upper or lower strands, coreSRF, Elk-1, and either Gal4-CBP(1–451) or Gal4-CBP(1100–1286) and subjected to a brief DNaseI digestion, and the purified DNA was analyzed by electrophoresis on a sequencing gel as above. The lower strand showed subtle differences in the DNaseI digestion pattern between the ternary complex and the bromocomplex. A hypersensitive site in the 3'-half of the SRE appears in the bromocomplex (Fig. 5, right, filled circle), and increased protection is apparent within and upstream of the TCF-binding site with the bromodomain relative to CBP(1–451) and TCF (Fig. 5, right, arrows). Under these conditions the ternary complex alone does not protect the lower strand from DNase I

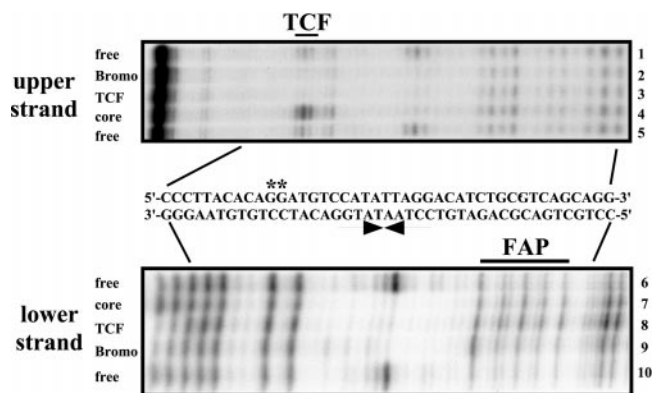


FIG. 4. Methylation interference analysis of binary, ternary, and bromocomplexes formed on the *c-fos* SRE. coreSRF·SRE, TCF·coreSRF·SRE, and Gal4-CBP(1100–1286)·TCF·coreSRF·SRE complexes were formed using partially methylated SRE probes labeled selectively on the upper or lower strands. The different complexes (see Fig. 2) were purified from the gel, and their methylation sensitivity was determined by piperidine cleavage of the isolated DNA and analysis on a 10% sequencing gel. The identity of the different complexes is shown on the left as is the probe strand being visualized. The sequence of the SRE probe is indicated between the two autoradiograms. The lines indicate the position of the corresponding residue on the gel, the arrows underlie the dyad-symmetrical core of SRE, and the asterisks show the two G residues on the upper strand contacted by TCF, also indicated by TCF above the upper strand autoradiogram.

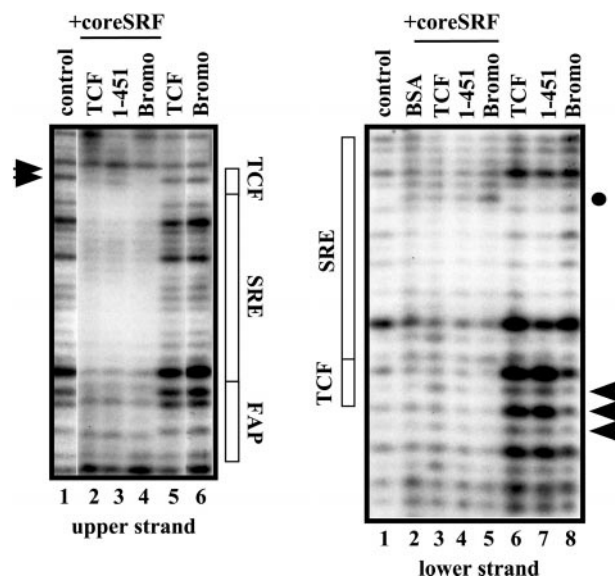


FIG. 5. DNase I footprint analysis of the bromocomplex. Binding reactions were assembled on SRE probes ³²P-labeled on the upper strand or lower strand as indicated. The reactions contained the following proteins: none (lane 1, right and left), coreSRF and BSA (lane 2, right), coreSRF and Elk-1 (lane 3, right; lane 2, left), coreSRF Elk-1 and Gal4-CBP(1–451) (lane 4, right; lane 3, left), coreSRF Elk-1 and Gal4-CBP(1100–1286) (lane 4, left; lane 5, right), Elk-1 (lane 5, left; lane 6, right), Gal4-CBP(1–451) (lane 7, right), Gal4-CBP(1100–1286) (lane 6, left; lane 8, right). After a short DNase I digestion, the fragments were purified and analyzed on a 10% sequencing gel as in Fig. 4. The positions of the TCF-binding site, SRF-binding site, and the FAP sequence are shown next to the autoradiograms. The arrowheads indicate sites protected in the bromocomplex, and the filled circle indicates the lower strand hypersensitive site in the bromocomplex.

but rather appears to increase its sensitivity (compare lanes 2 and 3, lower strand). No protection is seen with these proteins in the absence of coreSRF (Fig. 5, right). The upper strand shows the classic protection pattern conferred by the ternary complex (Fig. 5, left) (26). Interestingly, adding CBP(1100–1286), but not CBP(1–451), led to increased protection immediately upstream of the CAGG sequence contacted by TCF (10,

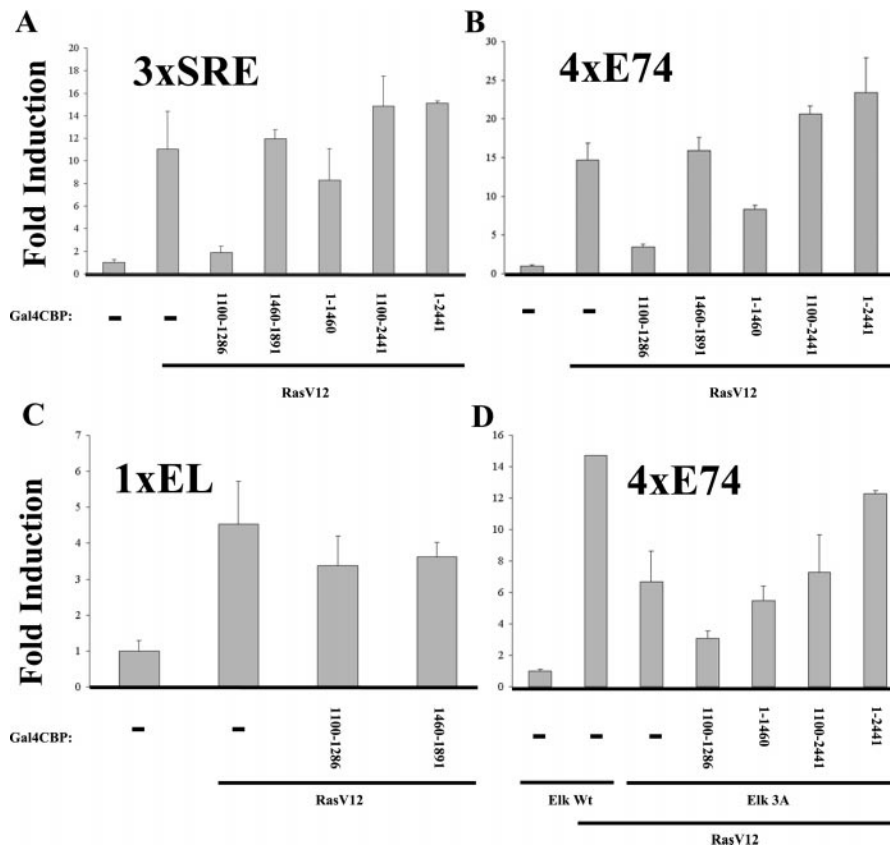


FIG. 6. The bromodomain of CBP represses RasV12-driven activation of SRE and E74 reporter genes in NIH3T3 cells. An expression vector for activated Ras (*RasV12*, 200 ng) was cotransfected with different Gal4-CBP expression vectors (1.5 μ g) into NIH3T3 cells together with a luciferase reporter gene (300 ng) driven by either three copies of the *c-fos* SRE (A), four copies of the E74 site (B and D), or a *c-fos* SRE mutated in the TCF-binding site (*EL*, C). A wt Elk-1 expression vector (50 ng) was cotransfected in B and D, as well as one for Elk-3A, with three alanine point mutations in the major MAPK phosphorylation sites, in D. The level of induction was calculated relative to the activity of the reporter in the absence of activation. The values represent the mean of duplicate or triplicate samples and are representative of at least three independent experiments.

26) and Elk-1 (20). (Fig. 5, left, arrows). As with the lower strand, CBP-(1100–1286) and TCF show the same DNase pattern as free DNA (Fig. 5, left, lanes 5 and 6). The bromocomplex also does not protect the FAP site downstream of the SRE (Fig. 5, left). Thus, the bromocomplex contains no obvious direct DNA contacts by the bromodomain, but rather protein-protein interaction with Elk-1 that seems to enhance Elk-1 binding to its recognition sequence.

CBP-(1100–1286) Represses SRE-driven Transcriptional Activation in NIH3T3 Cells—To investigate the potential functional significance of the bromocomplex, we measured its effect on SRE-driven reporter genes in transient transfection assays. In nonstimulated NIH3T3 cells, a 3xSRE luciferase reporter gene shows weak activity that is unaffected by cotransfecting Gal4-CBP-(1100–1286) (not shown). Ras-mediated signaling strongly induces SRE-driven gene expression, thus we tested the effect of different CBP expression vectors together with activated Ras (*RasV12*) on the activity of a 3xSRE luciferase reporter gene in these cells. The bromodomain strongly diminished SRE activation by *RasV12*, an effect not seen with other CBP regions (Fig. 6A). This repressive effect suggests that the bromodomain of CBP, on its own, can repress SRE activity under induced conditions. This was not surprising, because the molecule lacks both the N- and C-terminal activation domains that potentiate SRE activity in transfected cells (12–14). To test whether the activation domains could reverse this inhibition, we transfected the following expression vectors: CBP-(1–1460), which contains, 1) the N-terminal transactivation domain, 2) the region spanning aa 451–721 that interacts with the TCF C-terminal transactivation domain, 3) the SRF-inter-

acting module, 4) the bromodomain (but not the histone acetyltransferase domain immediately downstream) CBP-(1100–2441), which contains, 1) the bromodomain, 2) the histone acetyl transferase activity, 3) the C-terminal transactivation domain; CBP-(1–2441), the full-length CBP protein. These different proteins relieved the repressive effect of the bromodomain. CBP-(1–1460) showed an intermediate effect, whereas CBP-(1100–2441) restored reporter activity to nonrepressed levels. Surprisingly, CBP-(1–2441) was not significantly more effective than the CBP-(1100–2441) in potentiating transcriptional activity (Fig. 6A).

We then performed the same experiments with a 4xE74-luciferase construct to investigate the functional role of the bromocomplex in the absence of SRF (Fig. 6B). This consensus Ets-binding site is, like the SRE, targeted by Ras-mediated signaling. Because this reporter shows a high background due to its recognition by endogenous Ets-proteins (21), we cotransfected an Elk-1 expression vector. The same pattern was observed as with the SRE. The bromodomain led to a significant decrease in *RasV12*-dependent activation, an effect that again was not seen with other Gal4-CBP fusions. The addition of the N- or C-terminal transactivation domains of CBP (Gal4-CBP 1–1286, 1100–2441, and 1–2441) showed essentially the same relief of repression as with the SRE reporter.

Because the bromocomplex does not form on the SRE mutant EL where the binding of TCF is abolished, we used an EL-driven luciferase reporter gene to test for nonspecific inhibition by CBP-(1100–1286) (Fig. 6C). It has been shown that SRF alone can mediate SRE-driven transcriptional activation in a pathway dependent on the Rho/Rac/CDC42 family of small G

proteins (27). This reporter gene, as well as one containing three copies of the EL-SRE, was unaffected by cotransfection with the CBP-(1100–1286) expression vector, ruling out non-specific inhibition. Curiously, the EL reporter was also not activated by the CBP-(1–1460) expression vector containing the domain described to interact with SRF (14). Thus, this putative interaction is not sufficient to mediate transactivation in our conditions. Altogether, these data further confirm that the bromodomain of CBP is interacting with the TCF Elk-1 and not directly with SRF.

Elk-1 is strongly phosphorylated by MAPKs, and phosphorylation of serines 324, 383, and 389 is essential for transactivation (11). It has previously been shown that CBP-(451–721) interacts with the C-terminal domain of Elk-1 and that this interaction mediates Elk-1 transactivation (13). Our data suggested that bromocomplex formation *in vitro* did not require this interaction nor activated Elk-1. To test this functionally, we cotransfected the bromodomain, the 4xE74-luciferase reporter gene and an Elk-1 mutant where the three serine residues have been changed to alanine (Fig. 5D). Elk3A was still responsive to RasV12, although the level of activation was lower than *wt* Elk-1. Notably, the repressive effect of cotransfecting Gal4-CBP-(1100–1286) was still observed as was the rescue by the longer versions of Gal4-CBP fusions. Furthermore, the relative effects were similar to *wt* Elk-1. These data strongly suggest that bromodomain-driven interactions are independent of phosphorylation.

DISCUSSION

Our data present evidence for a novel regulatory complex on the *c-fos* SRE. This complex involves the interaction of the bromodomain of CBP with the ternary complex composed of SRF and TCF. Notably, these interactions seem to be independent of signaling that drives SRE activation. These conclusions are based on the following: 1) The bromodomain of CBP interacts with the C- and N-terminal regions of the TCF Elk-1 in solution. 2) The bromodomain forms a quaternary complex on the *c-fos* SRE together with SRF and Elk-1 *in vitro*. 3) The DNA-dependent *in vitro* interactions can be reconstituted on the Ets protein binding site E74, where Elk-1 binds in the absence of SRF, suggesting a sole requirement for TCF in bromocomplex formation. 4) Methylation interference analysis of the bromocomplex reveals no absolute requirement for any particular residue, instead suggesting that it forms over the ternary complex. 5) In transient transfection assays, the bromodomain of CBP represses SRE and E74 reporter activity in the absence of the C- and N-terminal activation domains. This repression is relieved when these domains are added. Moreover, the repression is dependent on Elk-1.

The rapid signaling-dependent induction of *c-fos* transcription *in vivo* implies a high degree of compartmentalization of transcription factors/promoter complexes together with adaptors/coactivators within the nucleus. Our starting hypothesis was that the coactivator CBP may form a constitutive complex with the SRE. In our *in vitro* system, bromocomplex formation seems to be independent of activation, suggesting that recruitment of CBP by phosphorylated transcription factors may not be required for the initial association of CBP with promoters. The constitutive presence of CBP on the *c-fos* SRE might explain the stability of the ternary complex *in vivo* and the extremely rapid activation of *c-fos* transcription after stimulation. This stability has yet to be seen *in vitro* where the ternary complex dissociates rapidly (10).

When formed with coreSRF (aa 90–245), the bromocomplex shows faster mobility than the ternary complex. Nevertheless, the complex contains CBP-(1100–1286), Elk-1, and core SRF, suggesting that the quaternary complex is more compact than

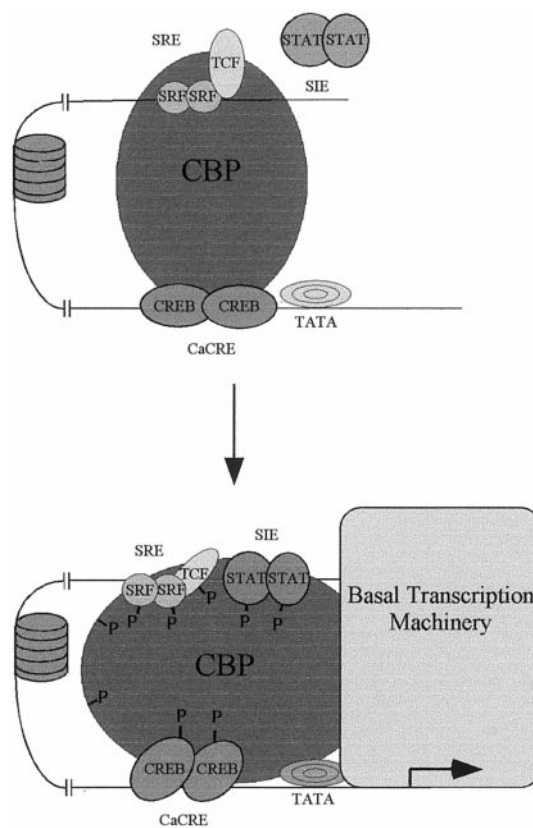


FIG. 7. **Model for the signaling-dependent transcriptional activation from the *c-fos* SRE.** The SRE is constitutively occupied by the ternary complex and CBP through interactions between the bromodomain of CBP and TCF. Signaling-driven phosphorylation of the proteins bound to the *c-fos* promoter elements would lead to a conformational change of CBP through interactions between different domains of CBP and these factors as described in Fig. 1A. This would allow CBP to contact the basal transcriptional machinery and potentiate transcriptional initiation.

the TCF·coreSRF ternary complex. In contrast, in the presence of full-length SRF, GST-Elk₃₀₇, or Elk-1 truncation mutants generated *in vitro*, the resulting bromocomplex migrates more slowly than does the ternary complex. In many instances the yield of the bromocomplex is increased relative to the ternary complex, but the basis for this increased efficiency is still unclear. The DNase footprints indicate that protection is increased around the TCF binding site in the bromocomplex. This suggests tighter binding by TCF in the complex. An additional component may involve changes in the conformation of the binding site, because the bromocomplex generates a hypersensitive site 3' in the SRE. These would also aid formation of a tighter, faster-migrating bromocomplex. Interestingly, this is only observed with Elk-1 expressed in mammalian cells, not with Elk-1 produced in bacteria or *in vitro*, which implies that post-translational modification contributes to this behavior.

Many factors, such as ATF-6, Phox-1, YY-1, C/EBP β , TFII-I, and ASC-2 have been reported to bind to or increase the efficiency of the SRF·SRE complex (28–36). The direct DNA requirement of these SRF-dependent interactions remains unclear, but in transient transfections they have been shown to variously activate or repress transcriptional activity. In contrast, the bromocomplex involves solely the TCF component of the ternary complex, because it showed identical behavior on the E74 site and on the SRE. Apparently, SRF is necessary for bromocomplex formation, because it is a prerequisite for ternary complex formation. The functional aspects of the bromocomplex are thus equally well studied by the SRE as well as the E74 element. It will be interesting to determine whether SRF

interacting factors that interact with SRF can synergize with CBP in the regulation of the SRE.

The homeoprotein Id also negatively affects TCF function *in vitro* and in transfected cells (37). In contrast to the mechanism we propose for the bromocomplex, Id interferes with DNA binding by Elk-1 and SAP-1a by acting on the Ets DNA binding domain. Similar to the bromodomain, Id overexpression blocks signaling-driven SRE activity. On the other hand, coexpression of Elk-1 rescues repression by Id but not by the bromocomplex (not shown). Thus Id and the bromodomain appear to repress SRE activity by distinct mechanisms involving TCF.

Our transient transfection results confirm that the bromocomplex can form on the *c-fos* SRE in culture cells. In the absence of the N- and C-terminal transactivation domains of CBP, the bromodomain repressed SRE- and E74-driven transcription, and this required an intact Elk-1-binding site on the SRE or coexpression of Elk-1 in the case of the E74 reporter. Thus, the bromodomain interferes with the ability of Elk-1 to transactivate. Expressing the bromodomain linked to the CBP transactivation domains facilitated activation, in agreement with previous studies (12–14). Janknecht and Nordheim (13) found that the KIX domain (aa 451–721) interacted with and potentiated MAPK-driven transactivation by the C-terminal region of Elk-1. Here we describe another interaction that involves other regions of both proteins. In particular, the interaction we describe is constitutive and not dependent upon signaling. It therefore could complement or synergize with other interactions between these two proteins.

The bromodomain of P/CAF (p300- and CBP-associated factor) has been described to function as a link between histones and histone acetylases (38). This raises the possibility that Elk-1 is also a target for these enzymes and that the interactions described here are dependent on acetylation. Our preliminary data indicate that endogenous Elk-1 may be acetylated, which would add a level of regulation independent of phosphorylation. Indeed, acetylation affects the enhanceosome on the *IFN- β* gene, where the protein HMG I(Y) is acetylated by CBP (39), leading to transcriptional repression. Interestingly, the SRE has been shown to have a centrally positioned nucleosome adjacent to the SRE (40), which likely contributes to the higher order structure of the promoter *in vivo* and may be target for acetylation. Our data suggest that the bromodomain could form a constitutive preinduction complex with the SRE via TCF. This would be consistent with the genomic footprint where a constitutive non-signaling-dependent complex is present on the *c-fos* SRE. The structural changes that occur upon activation of the *c-fos* promoter are most probably more complex than our transient transfection and *in vitro* binding assays suggest, considering the geometry of the promoter described by Herrera and coworkers (40). Nevertheless, our results are a first step toward a signaling-dependent functional and structural reconstitution of the *c-fos* promoter *in vitro*.

We present the following model for the signaling-driven transcriptional activation of the SRE. The SRE is constitutively occupied by the ternary complex and CBP *in vivo* (Fig. 7, *upper panel*). Signaling-driven phosphorylation of Elk-1, SRF, CREB, and STAT, as well as CBP itself (13), would drive a conformational change that permits the transactivation domains of CBP (both N- and C-terminal) to contact the basal transcription

machinery and thus potentiate the initiation of transcription (Fig. 7, *lower panel*). The bromocomplex would then constitute a key intermediate for the rapid induction of *c-fos* by a multitude of signals. Furthermore, the notion of a constitutive recruitment of bromodomain-containing coactivators, such as CBP and p300, to stable promoter complexes may also apply to other promoters depending on their respective coactivator and function.

Acknowledgments—We thank our colleagues in the Institut de Génétique Moléculaire de Montpellier, in particular the groups of C. Sardet and J.-M. Blanchard, for their advice and continued critical input during the course of these studies, R. Janknecht for the GST- and Gal4-CBP expression vectors, G. Bilbe and H. Richener for reporter gene constructs, and A. Philips for his invaluable counsel in the art of transient transfection.

REFERENCES

- Karin, M. (1994) *Curr. Opin. Cell Biol.* **6**, 415–424
- Treisman, R. (1996) *Curr. Opin. Cell Biol.* **8**, 205–215
- Hipskind, R. A., and Bilbe, G. (1998) *Front. Biosci.* **3**, D804–D816
- Gonzalez, G. A., and Montminy, M. R. (1989) *Cell* **59**, 675–680
- Xing, J., Kornhauser, J. M., Xia, Z., Thiele, E. A., and Greenberg, M. E. (1998) *Mol. Cell Biol.* **18**, 1946–1955
- Tan, Y., Rouse, J., Zhang, A., Cariati, S., Cohen, P., and Comb, M. J. (1996) *EMBO J.* **15**, 4629–4642
- Darnell, J. E., Jr. (1997) *Science* **277**, 1630–1635
- Treisman, R. (1995) *EMBO J.* **14**, 4905–4913
- Herrera, R. E., Shaw, P. E., and Nordheim, A. (1989) *Nature* **340**, 68–70
- Shaw, P. E., Schroter, H., and Nordheim, A. (1989) *Cell* **56**, 563–572
- Treisman, R. (1994) *Curr. Opin. Genet. Dev.* **4**, 96–101
- Janknecht, R., and Nordheim, A. (1996) *Oncogene* **12**, 1961–1969
- Janknecht, R., and Nordheim, A. (1996) *Biochem. Biophys. Res. Commun.* **228**, 831–837
- Ramirez, S., Ait-Si-Ali, S., Robin, P., Trouche, D., and Harel-Bellan, A. (1997) *J. Biol. Chem.* **272**, 31016–31021
- Kim, H. J., Kim, J. H., and Lee, J. W. (1998) *J. Biol. Chem.* **273**, 28564–28567
- Chrivia, J. C., Kwok, R. P., Lamb, N., Hagiwara, M., Montminy, M. R., and Goodman, R. H. (1993) *Nature* **365**, 855–859
- Zhang, J. J., Vinkemeier, U., Gu, W., Chakravarti, D., Horvath, C. M., and Darnell, J. E., Jr. (1996) *Proc. Natl. Acad. Sci. U. S. A.* **93**, 15092–15096
- Horvai, A. E., Xu, L., Korzus, E., Brard, G., Kalafus, D., Mullen, T. M., Rose, D. W., Rosenfeld, M. G., and Glass, C. K. (1997) *Proc. Natl. Acad. Sci. U. S. A.* **94**, 1074–1079
- Zinck, R., Hipskind, R. A., Pingoud, V., and Nordheim, A. (1993) *EMBO J.* **12**, 2377–2387
- Hipskind, R. A., Rao, V. N., Mueller, C. G., Reddy, E. S., and Nordheim, A. (1991) *Nature* **354**, 531–534
- Janknecht, R., and Nordheim, A. (1992) *Nucleic Acids Res.* **20**, 3317–3324
- Philips, A., Chambeyron, S., Lamb, N., Vie, A., and Blanchard, J. M. (1999) *Oncogene* **18**, 6222–6232
- Hipskind, R. A., Baccarini, M., and Nordheim, A. (1994) *Mol. Cell Biol.* **14**, 6219–6231
- Maxam, A. M., and Gilbert, W. (1980) *Methods Enzymol.* **65**, 499–560
- Vanhoutte, P., Nissen, J. L., Brugg, B., Della Gaspera, B., Besson, M. J., Hipskind, R. A., and Caboche, J. (2000) *J. Biol. Chem.*, in press
- Shaw, P. E. (1992) *EMBO J.* **11**, 3011–3019
- Hill, C., Wynne, J., and Treisman, R. (1995) *Cell* **81**, 1159–1170
- Zhu, C., Johansen, F. E., and Prywes, R. (1997) *Mol. Cell Biol.* **17**, 4957–4966
- Ryan, W. A., Jr., Franza, B. R., Jr., and Gilman, M. Z. (1989) *EMBO J.* **8**, 1785–1792
- Natesan, S., and Gilman, M. (1995) *Mol. Cell Biol.* **15**, 5975–5982
- Graham, R., and Gilman, M. (1991) *Science* **251**, 189–192
- Sealy, L., Malone, D., and Pawlak, M. (1997) *Mol. Cell Biol.* **17**, 1744–1755
- Hanlon, M., and Sealy, L. (1999) *J. Biol. Chem.* **274**, 14224–14228
- Kim, D. W., Cheriya, V., Roy, A. L., and Cochran, B. H. (1998) *Mol. Cell Biol.* **18**, 3310–3320
- Kim, D. W., and Cochran, B. H. (2000) *Mol. Cell Biol.* **20**, 1140–1148
- Lee, S. K., Na, S. Y., Jung, S. Y., Choi, J. E., Jhun, B. H., Cheong, J., Meltzer, P. S., Lee, Y. C., and Lee, J. W. (2000) *Mol. Endocrinol.* **14**, 915–925
- Yates, P. R., Atherton, G. T., Deed, R. W., Norton, J. D., and Sharrocks, A. D. (1999) *EMBO J.* **18**, 968–976
- Dhalluin, C., Carlson, J. E., Zeng, L., He, C., Aggarwal, A. K., and Zhou, M. M. (1999) *Nature* **399**, 491–496
- Munshi, N., Merika, M., Yie, J., Senger, K., Chen, G., and Thanos, D. (1998) *Mol. Cell* **2**, 457–467
- Herrera, R. E., Nordheim, A., and Stewart, A. F. (1997) *Chromosoma* **106**, 284–292